nature biotechnology

SUPPLEMENTARY INFORMATION

https://doi.org/10.1038/s41587-019-0207-y

In the format provided by the authors and unedited.

Immuno-SABER enables highly multiplexed and amplified protein imaging in tissues

Sinem K. Saka[1,2,11]*, Yu Wang[1,2,3,11]*, Jocelyn Y. Kishi[1,2], Allen Zhu[1,2], Yitian Zeng[1,3], Wenxin Xie[1,3], Koray Kirli[4], Clarence Yapp[5,6], Marcelo Cicconet[5], Brian J. Beliveau[1,2,10], Sylvain W. Lapan[3], Siyuan Yin[1,3], Millicent Lin[1,3], Edward S. Boyden[7], Pascal S. Kaeser[8], German Pihan[9], George M. Church[1,3] and Peng Yin[1,2]*

[1]Wyss Institute for Biologically Inspired Engineering, Harvard University, Boston, MA, USA. [2]Department of Systems Biology, Harvard Medical School, Boston, MA, USA. [3]Department of Genetics, Harvard Medical School, Boston, MA, USA. [4]Department of Biomedical Informatics, Harvard Medical School, Boston, MA, USA. [5]Image and Data Analysis Core, Harvard Medical School, Boston, MA, USA. [6]Laboratory of Systems Pharmacology, Harvard Medical School, Boston, MA, USA. [7]Media Lab, Massachusetts Institute of Technology (MIT), Cambridge, MA, USA. [8]Department of Neurobiology, Harvard Medical School, Boston, MA, USA. [9]Pathology Department, Beth Israel Deaconess Medical Center, Boston, MA, USA. [10]Present address: Department of Genome Sciences, University of Washington, Seattle, WA, USA. [11]These authors contributed equally: Sinem K. Saka, Yu Wang. *e-mail: sinem.saka@wyss.harvard.edu; yuwang01@fas.harvard.edu; py@hms.harvard.edu

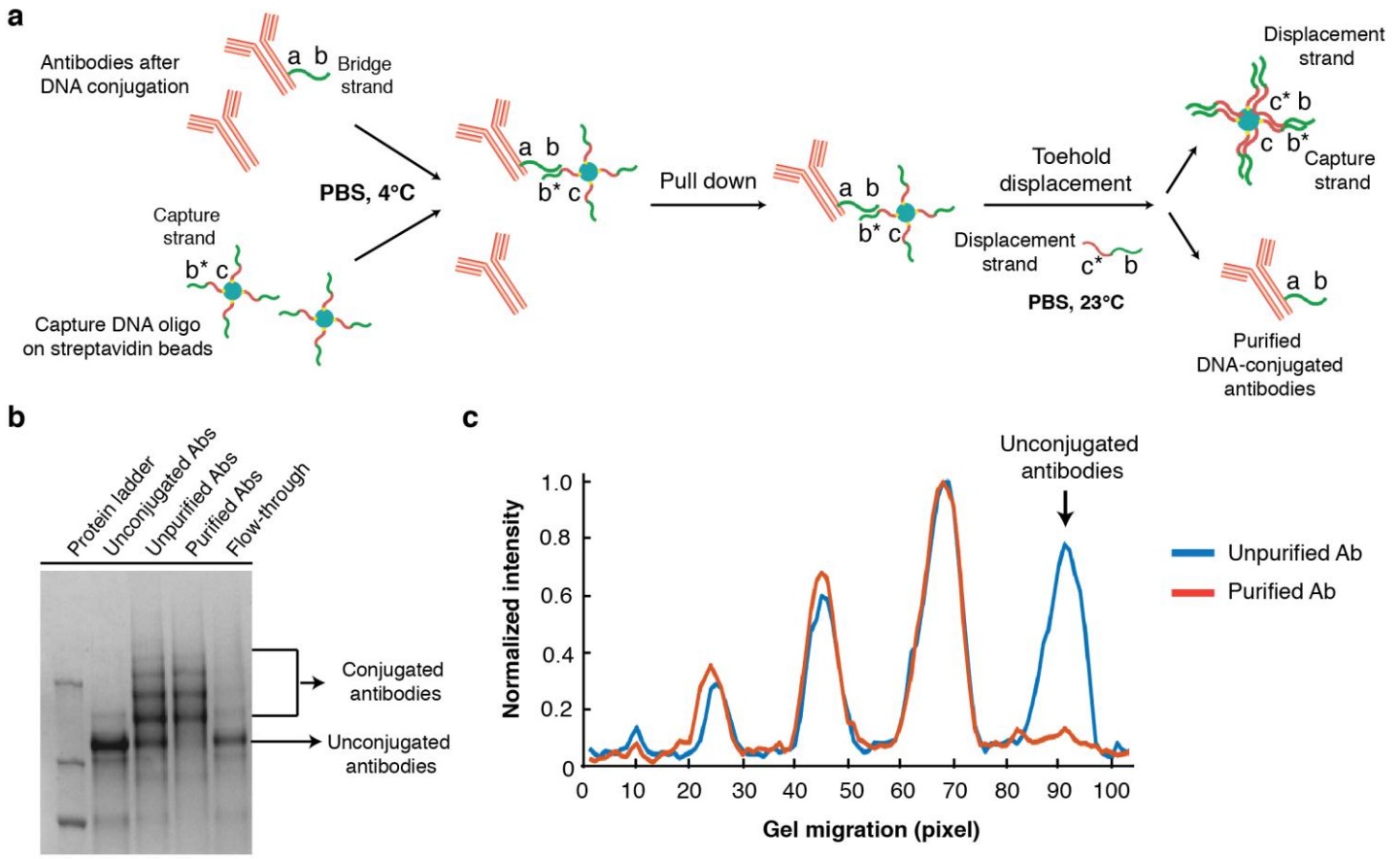

Supplementary Figure 1

Optional purification of DNA-conjugated antibodies using a toehold displacement-mediated DNA affinity pull-down.

(a) Schematic of the pull down assay. Biotin-modified capture DNA strands (biotin-*c*-*b**, where *c* is 15-nucleotides and *b** is 16-nucleotides) are attached to streptavidin beads, and used to pull down DNA-conjugated antibodies after antibody-bridge DNA conjugation (bridge strand sequence: *a*-*b,* where *b* is 16 nucleotides). The attached antibodies are dissociated from the beads using toehold displacement strands (*c**-*b*) that compete with the capture strands (Zhang and Winfree, 2009) on antibodies. While optional for Immuno-SABER, we found that purifying the DNA-conjugated antibodies via pull-down and toehold-mediated displacement may be helpful to improve the signal for select antibodies. **(b)** Visualization of purification products using an SDS-PAGE gel assay. After DNA conjugation, the majority of antibodies were conjugated with 0, 1 or 2 DNA oligos per antibody. After purification, antibodies without DNA were removed. **(c)** Plot of protein densities for the bands in **b**. The band corresponding to the removed unconjugated antibodies is marked with an arrow.

Reference: Zhang, D.Y. & Winfree, E. Control of DNA strand displacement kinetics using toehold exchange. J Am Chem Soc 131, 17303-17317 (2009).

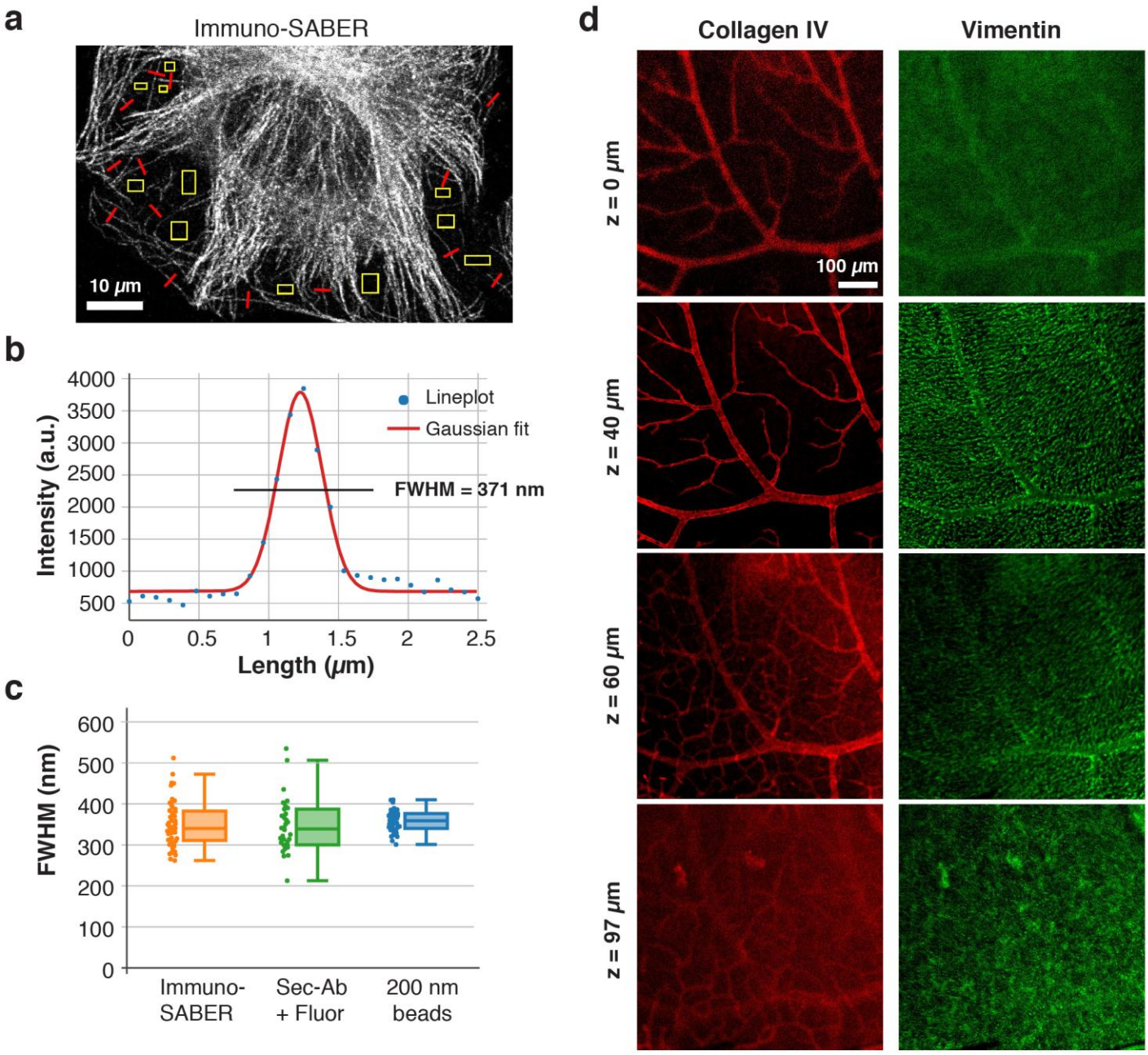

Supplementary Figure 2

Resolution and penetration controls for Immuno-SABER.

(a) ~2.5 µm long lineplots (red) were made over the thin tubules to estimate the observed resolution. Yellow-boxed background regions were used to estimate the background for subtraction. **(b)** A typical line plot along a tubule and the Gaussian fit, where full-width-half-maximum (FWHM) was calculated as 371 nm. **(c)** Mean FWHM values were calculated for 30-45 lineplots from cells stained with Immuno-SABER or fluorophore-conjugated secondary antibodies samples and the distribution was displayed as a box plot. A similar calculation was performed for 200 nm fluorescent beads. Mean FWHM was not significantly different (p value is 0.360 for Immuno-SABER and 0.335 for conventional secondary antibody staining, two-sample t-test comparison to the bead sample). Box-plots are drawn with center line, median; box limits, upper and lower quartiles; whiskers, min and max values capped at 1.5× interquartile range. **(d)** Visualization of Collagen IV and Vimentin at multiple depths of the whole mount mouse retina shown in **Fig. 2f**. Selected confocal planes are shown. Vimentin stains the Muller cells and Collagen IV stains the blood vessels, both of which are localized predominantly in the segments from nerve fiber layer to outer plexiform layer (~100 µm) of the retina (Slijkerman et al., 2015). Hence it should be noted that, although the entire whole-mount retina is about ~180 µm, the target signal comes from roughly one half of the

retina section, from the nerve fiber layer to the outer plexiform layer.

Reference: Slijkerman, R.W. et al. The pros and cons of vertebrate animal models for functional and therapeutic research on inherited retinal dystrophies. Prog Retin Eye Res 48, 137-159 (2015).

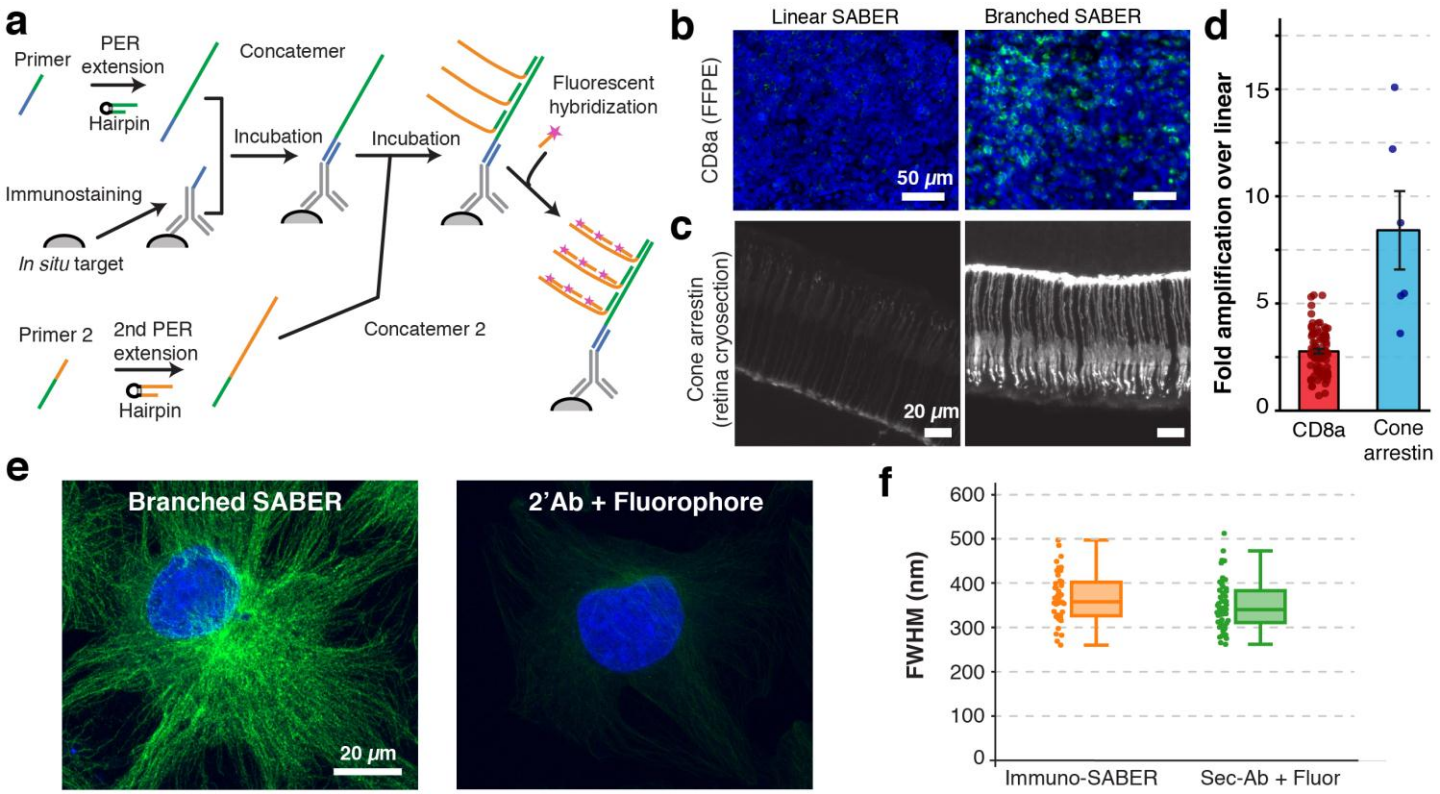

Supplementary Figure 3

Higher signal amplification via branching.

(a) Primary PER concatemers can be targeted by secondary concatemers to form a branched structure which amplifies the signal further by presenting additional binding sites for the imagers. **(b-c)** Representative images for linear and branched SABER amplification are shown for different preparations: **(b)** CD8a staining in human tonsil FFPE sections (single plane large area scans with 20× objective, cropped to show a CD8a-rich interfollicular zone region, **(c)** Cone arrestin staining in mouse retina cryosections (max projections from confocal *z* stacks). **(d)** Level of signal amplification by branched Immuno-SABER over linear was quantified by measuring the background-subtracted mean fluorescence for several regions of interest in the tissues and expressed as fold amplification over linear SABER. For CD8a FFPEs, n = 144 (for linear) and 84 (for branched) rectangular ROIs (each covering 0.03-1.20 mm^2 tissue regions; consecutive sections are used for the two conditions). For cone arrestin, n = 6 images from 2 retina samples. Error bars, s.e.m. **(e)** Alpha-tubulin staining (Alexa647) in cultured BS-C-1 cells (max projections from confocal *z* stack). **(f)** Mean FWHM values were calculated for 43 lineplots from cells stained with branched Immuno-SABER. For comparison values for conventional staining is also included. Box-plots are drawn with center line, median; box limits, upper and lower quartiles; whiskers, min and max values capped at 1.5× interquartile range. Mean FWHM for branching was not significantly different than the sub-diffraction 200 nm bead samples (plotted in **Supplementary Fig. 2c**) (p value is 0.303, two-sample t-test comparison to the bead sample).

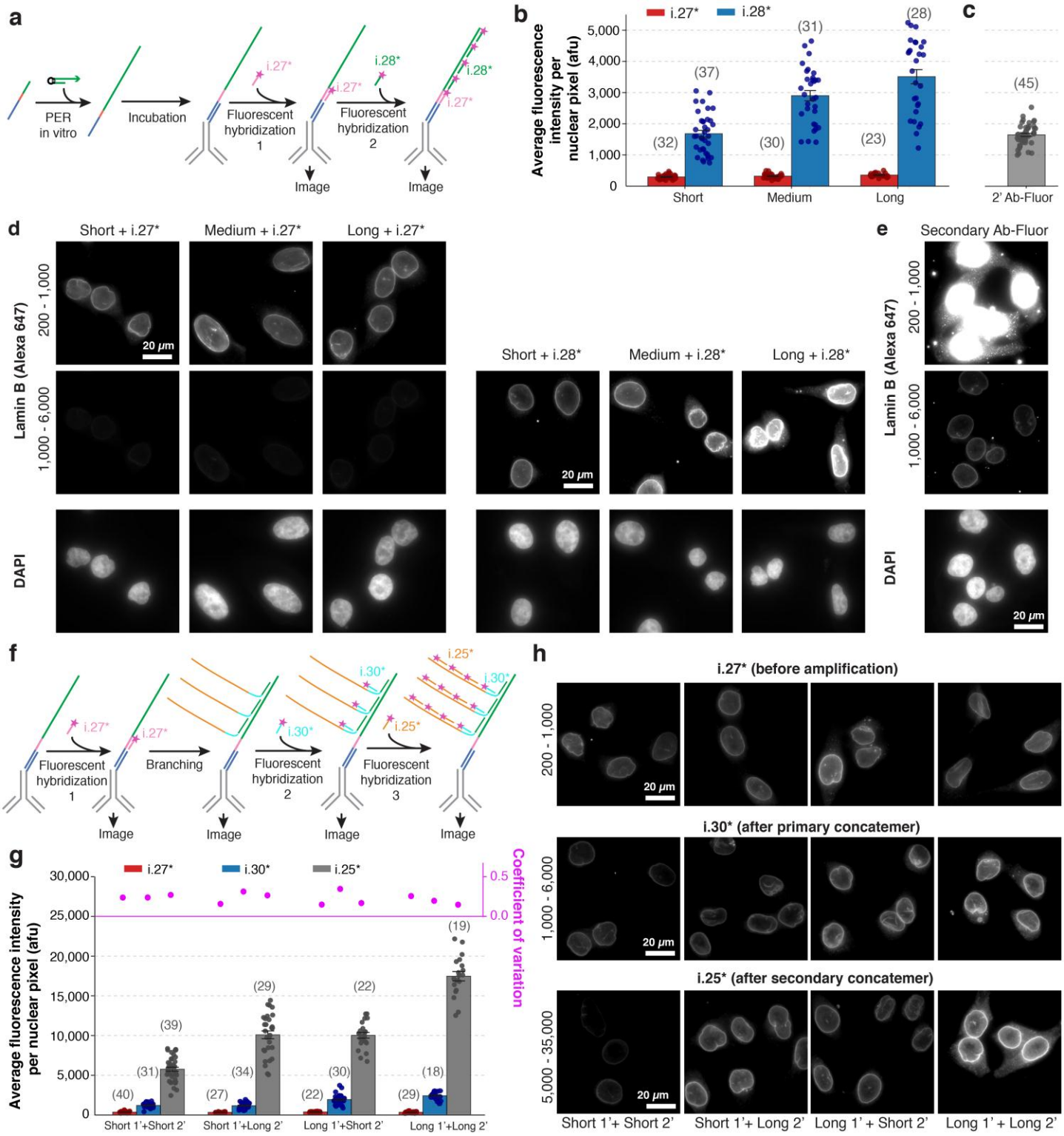

Supplementary Figure 4

Accessibility, concatemer length, and quantitativeness controls for Immuno-SABER.

(a) Experiment design: HeLa cell preparations were stained with anti-Lamin B antibodies and oligo-conjugated secondary antibodies. Concatemers of different sizes (short: 350 nt, medium: 450 nt, long: 700 nt, length estimations are based on the gel run with respect to

dsDNA ladder) were then hybridized to the antibodies. For this case, concatemers that contain an extra orthogonal binding site (for i.27*, as baseline imager) before the primer domain (p.28) were utilized. Samples were imaged first with only the baseline imager, then with the amplifier imager (i.28*). Imaging was done at 100× and 22-25 plane *z* stacks were acquired by an epifluorescence microscope. **(b)** Nuclei were segmented based on DAPI and mean Lamin B fluorescence intensity per nuclear pixel was calculated. n = 23-45 cells (individual sample sizes are written in parenthesis above each bar). Error bars, s.e.m. **(c)** For reference, the same target was also stained with commercial fluorophore-conjugated secondaries that on average bear 5× Alexa647 fluorophores and the fluorescence was measured the same way. **(d)** Representative images show the maximum projections for DAPI and Lamin B staining (Alexa647) for baseline and amplification conditions. The intensity scaling for each row is note on the left-hand side. **(e)** Secondary antibody-fluorophore images are shown for comparison. **(f)** Branching experiment design: A separate set of cells were similarly imaged with the baseline imager after hybridization of short (350 nt) or long primary concatemers (700 nt). This was followed by hybridization of secondary concatemers (short: 250 nt, long: 450 nt). Secondary concatemers also contained an orthogonal binding site (for i.30*) before the primer domain (p.25*). Baseline for branching (post-linear) was imaged by i.30*, followed by branched amplification with i.25*. **(g)** Lamin B fluorescence intensity per nuclear pixel was calculated as in **b** and is shown with the bar plot (left axis) overlaid with the scatter plot showing the distribution in the dataset. The dot plot above (magenta, right axis) shows the coefficient of variation for all the conditions. Note that the imagers bind dimers of primer units, whereas branches bind trimers for higher stability during exchange rounds. Therefore compared to the i.28* staining in previous panels, i.30* is expected to yield 1.5-fold lower signal (blue bars in **b** and **g**). **(h)** Representative images show the maximum projections corresponding to the conditions in **g**. All images are acquired under comparable conditions, and are displayed at the given intensity scaling for each amplification level.

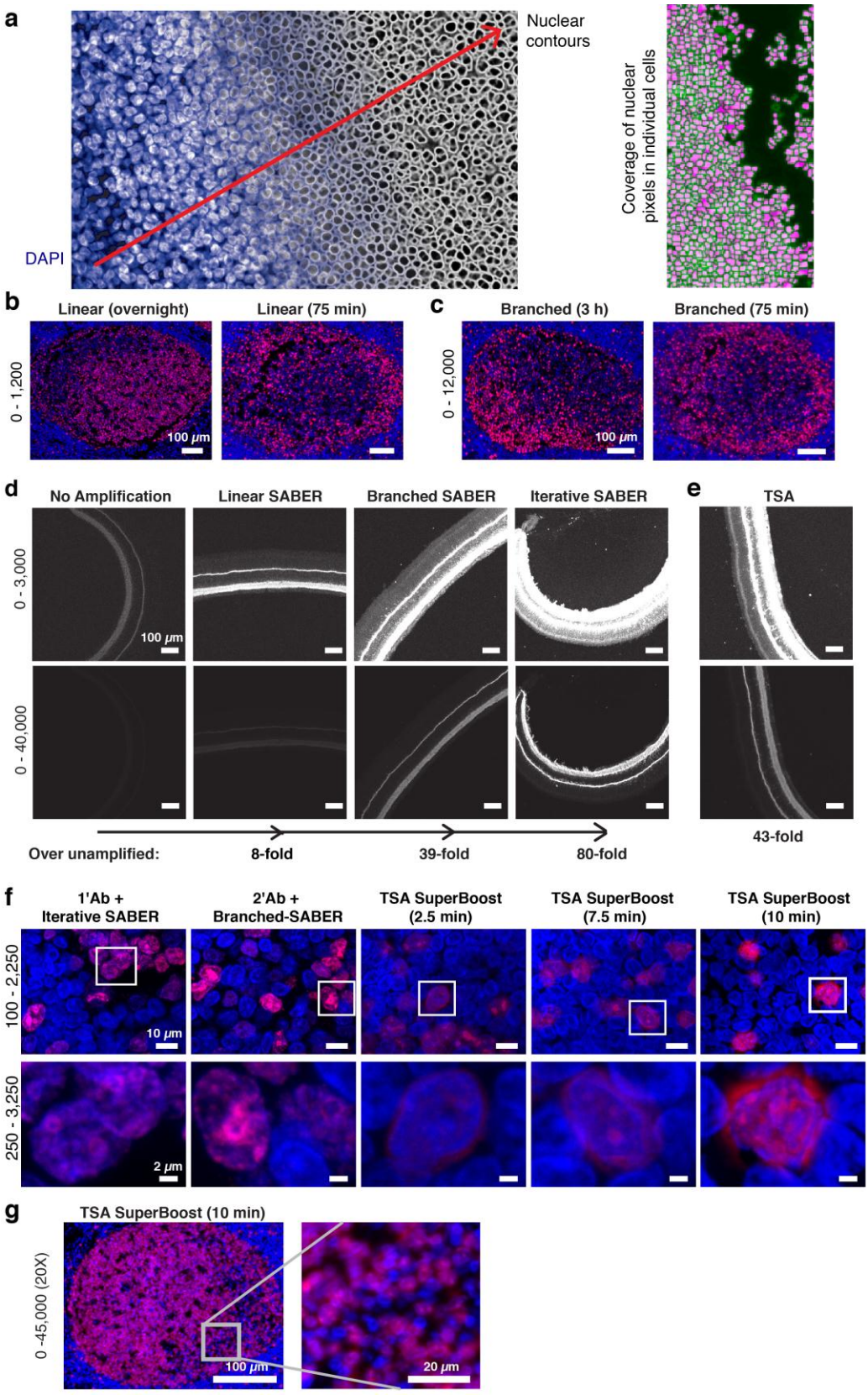

Supplementary Figure 5

Additional images for branching.

(a) Machine-learning based nucleus segmentation for signal quantification: The deep learning model was trained with a manually annotated dataset to enable automatic identification of nuclear contours to be followed by watershed segmentation. The image highlights nuclear contours (right side of the image) from DAPI staining (left side). Right panel: Watershed segmentation was used to segment (pink) the pixels corresponding to nuclei of each cell**. (b-c)** Images display a typical germinal center in human FFPE tonsil samples stained for Ki-67 (Alexa647, red) by Immuno-SABER. DAPI stain (blue) is shown for reference. Qualitatively similar amplification levels were obtained by long and short hybridization times (at 37°C) for the primary concatemer and branching concatemer (75 min each). **(d)** Iterative SABER of SV2 (Alexa647) in a 40 μm mouse retina cryosection. **(e)** For comparison SV2 staining with TSA was performed using mono HRP conjugated secondary antibodies. **(f)** Zoom-out and zoom-in views of the high-magnification confocal images in **Fig. 3f** displayed at different scaling ranges for comparative visualization. 10 min TSA amplification is included for further comparison. **(g)** Application of tyramide-Alexa647 for the maximum recommended incubation of 10 min. The germinal center image on the left is scaled in the same range with **Fig. 3d**. Zoom-in on the right is included to display the significant blurring of the signal at 10 min incubation.

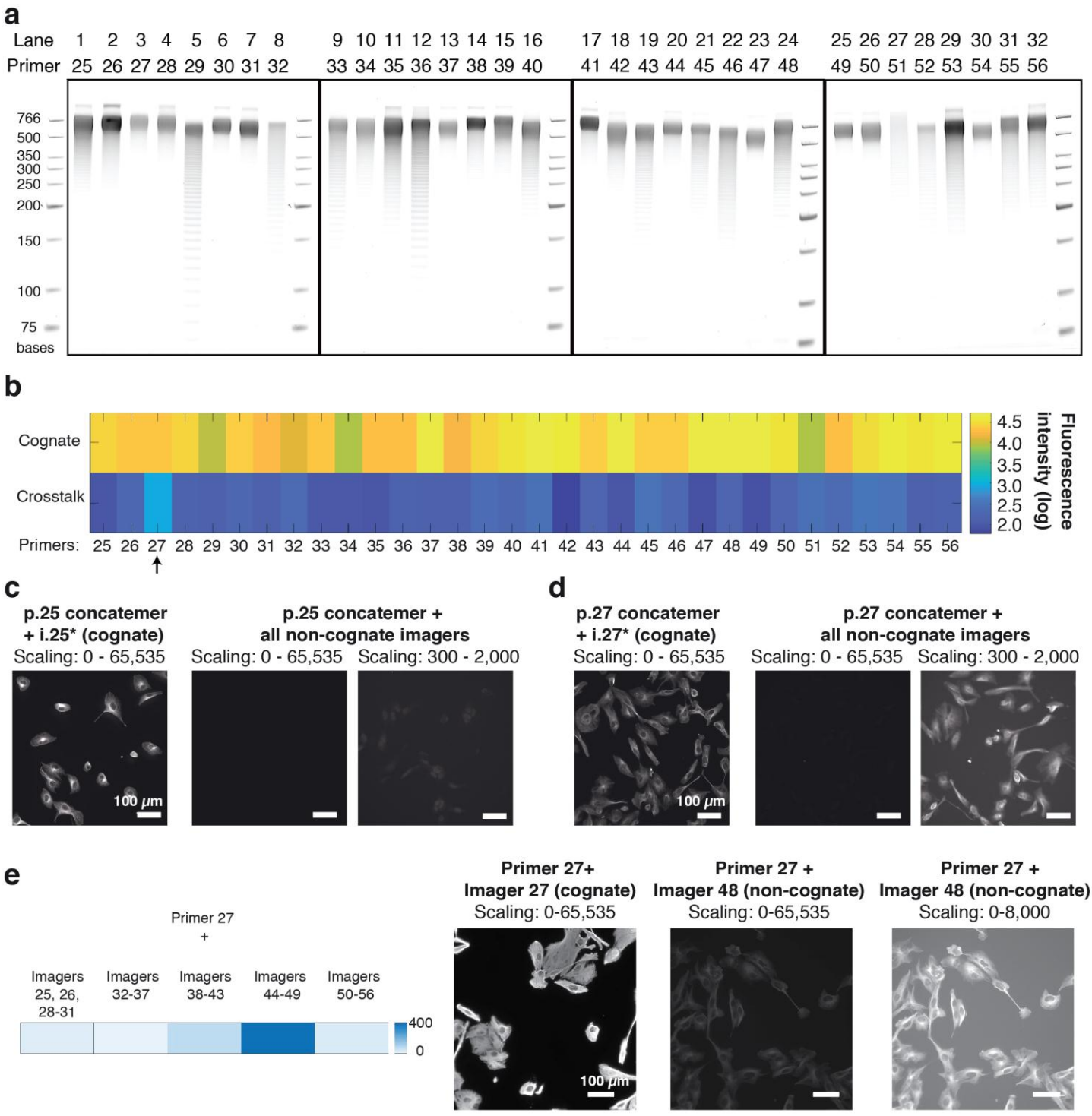

Supplementary Figure 6

Sequence validation for Exchange-SABER.

(a) 32 SABER sequences were extended to ~650 bases *in vitro* and examined by gel shift assay visualized with SybrGold on 6% denaturing PAGE gels. Qualitatively, 18 of the 32 sequences (such as #29) displayed a broader distribution with a ladder of shorter products visible albeit these bands being much dimmer than the predominant concatemer band. Although being extended, one sequence (#51) had a more even distribution in the upper length regime without a clear predominant band. Based on these

distributions, particular applications may favor a subset of the sequence library, i.e. high efficiency primers (for example primers 27, 28, 30, 31, 37, 38, 41, 44, 47, 49, 50, 54) may be more favorably utilized for more quantitative experiments or for lower abundance proteins. **(b-d)** *In situ* performance and crosstalk analysis. BS-C-1 cells were stained with bridge DNA-conjugated antibodies targeting α-Tubulin on a 96-well plate. Concatemers extended from each primer were hybridized to the bridges creating an array of wells labeled with primer sequences p.25-p.56. For each concatemer two sets of wells were prepared: (i) cognate group to be incubated with the corresponding imager strands, and (ii) crosstalk group where we added mixtures of imagers except the cognate imager strand. For each primer (e.g. p.25), both cognate and crosstalk wells were prepared by either applying the corresponding Alexa647-imager (e.g. i.25*) or all the imagers except the cognate one (e.g. -i.26* to i.56*). Images were captured in 16-bit (0-65,535). Representative images are shown for Primer 25 (p.25) **(c)** and Primer 27 (p.27) concatemers **(d)**. Crosstalk images are displayed with two different intensity scales to render the crosstalk signal visible. The fluorescence signals were quantified and plotted in the log scale and displayed as a heatmap. Consistent with the *in vitro* gel shift assay in panel **a**, sequences that had lower extension efficiency (particularly primers 29, 32, and 51) tended to yield less fluorescence signal compared to sequences that that extend with higher efficiency. Non-negligible crosstalk signal was only detected for Primer 27 concatemer (red box). **(e)** Crosstalk analysis of primer sequence p.27. BS-C-1 cells were fixed and stained with DNA-conjugated antibodies targeting alpha-Tubulin. Concatemers extended from primer sequence p.27 were hybridized to the antibodies, followed by addition of non-cognate imager strands. We first grouped every five imager strands and determined that p.27 had crosstalk with imager 44-49. We then tested individual imager strands from imager 44-49 and determined the strand responsible for crosstalk as imager strand 48 (i.48*), which is excluded from the library for further multiplexed imaging in presence of p.27.

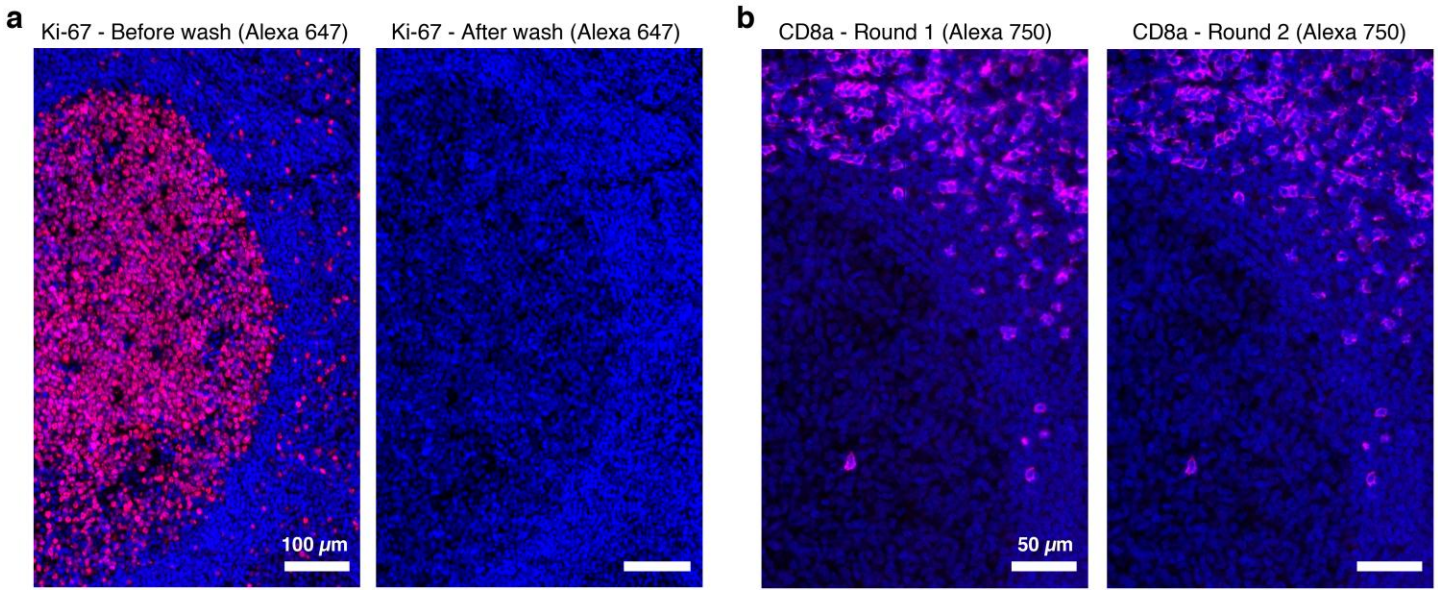

Supplementary Figure 7

Controls for exchange imaging of FFPE human tonsil sections.

(a) Imagers can efficiently removed within 10 min by washing the sample with 50% formamide in PBS, as shown in before and after wash images of the same section stained for Ki-67 (red) with linear amplification, imaged and displayed under the same conditions. DAPI stain is shown in blue. **(b)** Under this wash condition (10 min with 50% formamide in PBS at RT) the concatemers are not displaced, as shown by exchange imaging of CD8a by re-binding the imagers to the same target and re-imaging the tissue section (linear amplification).

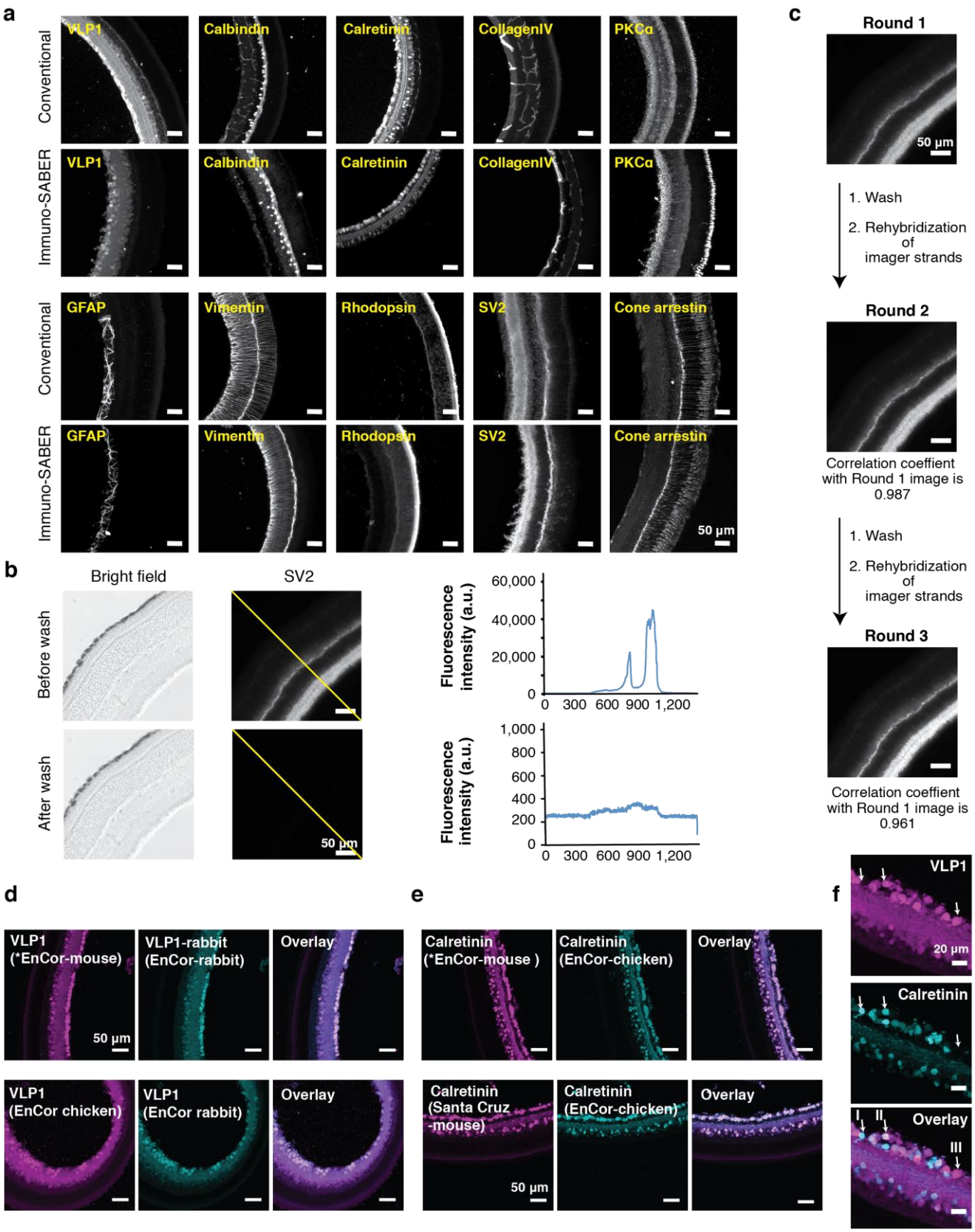

Supplementary Figure 8

Control experiments for highly multiplexed imaging in mouse retina sections.

(a) Comparison of antibody staining patterns before and after DNA conjugation. The images for unconjugated antibodies were taken using conventional fluorophore-conjugated secondary antibody labeling, and the images for antibodies after conjugation were taken using primary antibody-Immuno SABER labeling (images are displayed at individual contrast levels). **(b)** Efficiency of washing to remove the imager strands. A 30 μm mouse retina section was stained with DNA-conjugated SV2 antibodies and imaged using Alexa647-i.26* imager with a widefield microscope. Imager strands were washed using 0.1× PBS with 30% formamide at room temperature for 3×10 min. Before and after images were taken using the same imaging setting. The fluorescence intensity of indicated yellow line was measured using FIJI. **(c)** Washing conditions maintained sample integrity without signal loss. SV2 in mouse retina sections was imaged for 3 rounds and the correlation coefficient was calculated. The correlation coefficient between the images was above 0.95, suggesting the washing condition is sufficiently mild and non-disruptive. **(d-e)** Validation of the VLP1 and calretinin antibodies with conventional indirect immunostaining: The VLP1 (EnCor-mouse) and calretinin (EnCor-mouse) that were used for the multiplexing experiments (marked with asterisk) in **Fig. 5** were tested for specificity by co-staining with other antibodies targeting the same targets, followed by visualization using fluorophore-conjugated secondary antibodies. **(f)** Three cell subtypes (marked with arrows, I: $VLP1^{+}$ and $Calretinin^{+}$, II: $VLP1^{-}$ and $Calretinin^{+}$, III: $VLP1^{+}$ and $Calretinin^{-}$) identified in the multiplexed mouse retina imaging experiment were verified using conventional immunostaining with unconjugated primary antibodies (VLP1 by EnCor-rabbit and Calretinin by EnCor-mouse) and fluorophore-conjugated secondary antibodies.

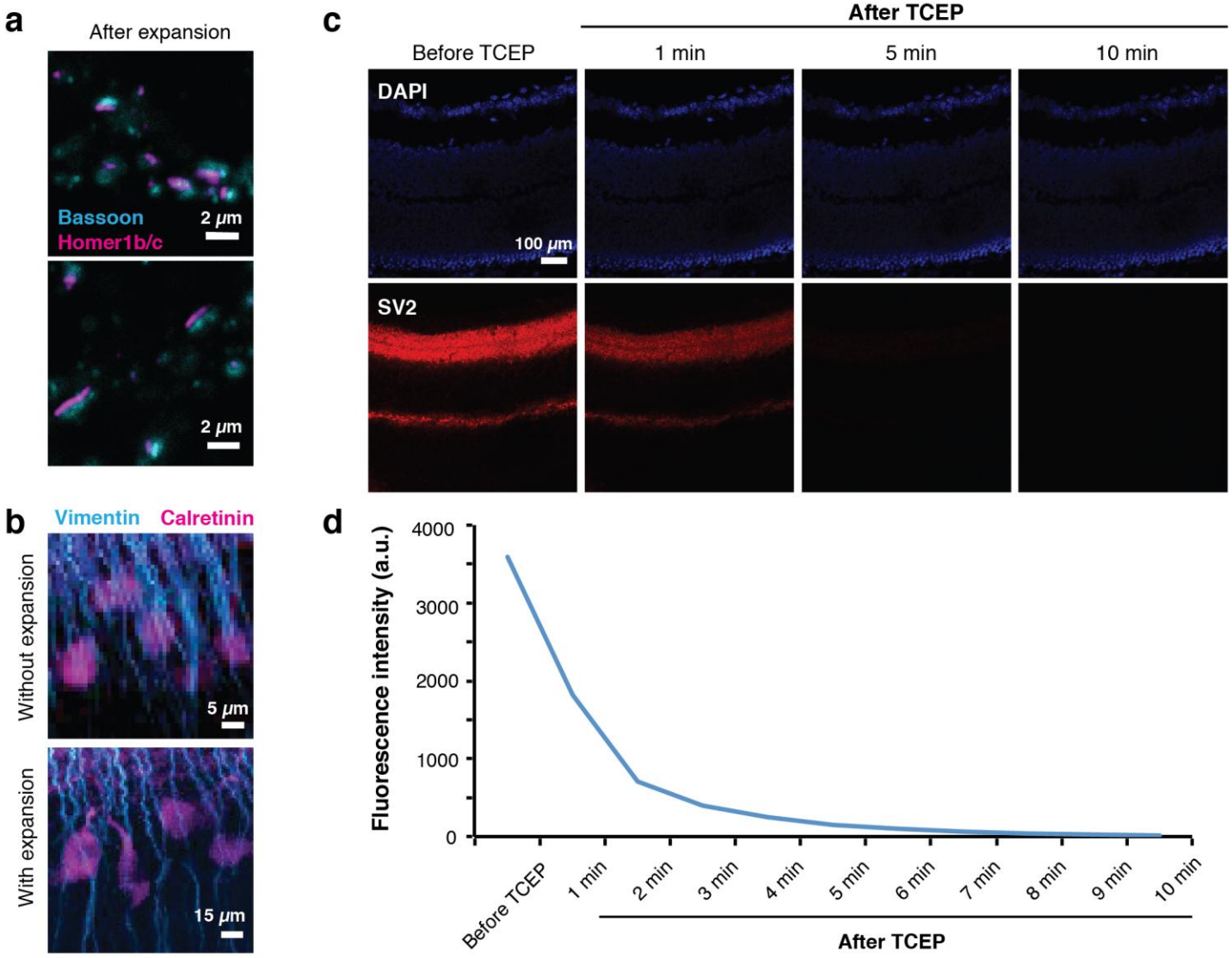

Supplementary Figure 9

Other sample orientations and alternative reduction-mediated fluorophore removal timeline for Expansion-SABER.

(a) Additional post-expansion images of neuronal synapses showing different orientations, as in **Fig. 6b**. **(b)** High-zoom comparison of Vimentin and Calretinin signals with and without expansion. The image with expansion is the overlay of the Vimentin and Calretinin images from **Fig. 6c**, whereas the image without expansion was derived from images in **Fig. 5a**. Scale bar indicates the physical size after expansion (~3-fold). **(c)** Alternative fluorophore removal strategy using TCEP reduction in thick expanded samples using TCEP. A mouse retina section stained with SV2 was expanded and visualized with disulfide bond modified imager strands. The fluorophores (Alexa 647) on the imager strands were cleaved using TCEP reduction. The fluorescence signal was monitored using a confocal microscope in a time course for 10 min. **(d)** Quantification of fluorescence signals in **c** before and after TCEP reduction.

Supplementary Tables

Supplementary Table 1. Optimized concatemer extension conditions and sequences for the primer library (for Supplementary Fig. 6).

Primer ID	Primer sequence	Hairpin ID	Hairpin sequence	Hairpin concentration	Time
p.25	CCAATAATA	h.25.25	ACCAATAATAGGGCCTTTTGGCCCTATTATT GGTTATTATTGG/3InvdT/	0.15 μM	3 h
p.26	ATAAACCTA	h.26.26	AATAAACCTAGGGCCTTTTGGCCCTAGGTTT ATTTAGGTTTAT/3InvdT/	0.9 μM	3 h
p.27	CATCATCAT	h.27.27	ACATCATCATGGGCCTTTTGGCCCATGATG ATGTATGATGATG/3InvdT/	0.075 μM	3 h
p.28	CAACTTAAC	h.28.28	ACAACTTAACGGGCCTTTTGGCCCGTTAAG TTGTGTTAAGTTG/3InvdT/	0.3 μM	2 h
p.29	TCTAAAATC	h.29.29	ATCTAAAATCGGGCCTTTTGGCCCGATTTTA GATGATTTTAGA/3InvdT/	0.15 μM	3 h
p.30	AATACTCTC	h.30.30	AAATACTCTCGGGCCTTTTGGCCCGAGAGT ATTTGAGAGTATT/3InvdT/	0.5 μM	2 h
p.31	TTATTCACT	h.31.31	ATTATTCACTGGGCCTTTTGGCCCAGTGAAT AATAGTGAATAA/3InvdT/	0.85 μM	2 h
p.32	CTTTTTTTC	h.32.32	ACTTTTTTTCGGGCCTTTTGGCCCGAAAAAA AGTGAAAAAAAG/3InvdT/	1.5 μM	3 h
p.33	CCTTCTATT	h.33.33	ACCTTCTATTGGGCCTTTTGGCCCAATAGAA GGTAATAGAAGG/3InvdT/	0.5 μM	2 h
p.34	CTCTACTAC	h.34.34	ACTCTACTACGGGCCTTTTGGCCCGTAGTAG AGTGTAGTAGAG/3InvdT/	0.4 μM	2 h
p.35	TAAAAACTC	h.35.35	ATAAAAACTCGGGCCTTTTGGCCCGAGTTTT TATGAGTTTTTA/3InvdT/	1.5 μM	3 h
p.36	AACTAATCT	h.36.36	AAACTAATCTGGGCCTTTTGGCCCAGATTA GTTTAGATTAGTT/3InvdT/	1 μM	2 h
p.37	TTTCTCTTC	h.37.37	ATTTCTCTTCGGGCCTTTTGGCCCGAAGAGA AATGAAGAGAAA/3InvdT/	0.85 μM	2 h
p.38	AACATACTA	h.38.38	AAACATACTAGGGCCTTTTGGCCCTAGTAT GTTTTAGTATGTT/3InvdT/	0.5 μM	2 h
p.39	TTCATTTAC	h.39.39	ATTCATTTACGGGCCTTTTGGCCCGTAAATG AATGTAAATGAA/3InvdT/	1 μM	2 h
p.40	ATCCTACAA	h.40.40	AATCCTACAAGGGCCTTTTGGCCCTTGTAG GATTTTGTAGGAT/3InvdT/	0.9 μM	2 h
p.41	CAATCAAAA	h.41.41	ACAATCAAAAGGGCCTTTTGGCCCTTTTGAT TGTTTTTGATTG/3InvdT/	0.45 μM	3 h
p.42	CTTACAAAC	h.42.42	ACTTACAAACGGGCCTTTTGGCCCGTTTGTA AGTGTTTGTAAG/3InvdT/	0.5 μM	2 h
p.43	ACAAATAAC	h.43.43	AACAAATAACGGGCCTTTTGGCCCGTTATTT GTTGTTATTTGT/3InvdT/	0.5 μM	2 h
p.44	TTTTCTACC	h.44.44	ATTTTCTACCGGGCCTTTTGGCCCGGTAGAA AATGGTAGAAAA/3InvdT/	0.45 μm	3h
p.45	CCCTTATTT	h.45.45	ACCCTTATTTGGGCCTTTTGGCCCAAATAAG GGTAAATAAGGG/3InvdT/	0.4 μM	3 h
p.46	TCTTTCATT	h.46.46	ATCTTTCATTGGGCCTTTTGGCCCAATGAAA GATAATGAAAGA/3InvdT/	0.45 μM	3 h
p.47	TTCTTACTC	h.47.47	ATTCTTACTCGGGCCTTTTGGCCCGAGTAAG AATGAGTAAGAA/3InvdT/	0.85 μM	1 h
p.48	CCATAAATC	h.48.48	ACCATAAATCGGGCCTTTTGGCCCGATTTAT GGTGATTTATGG/3InvdT/	0.4 μM	3 h

p.49	CATTTATCC	h.49.49	ACATTTATCCGGGCCTTTTGGCCCGGATAA ATGTGGATAAATG/3InvdT/	0.65 µM	1 h
p.50	ATACTTCAC	h.50.50	AATACTTCACGGGCCTTTTGGCCCGTGAAG TATTGTGAAGTAT/3InvdT/	0.4 µM	1 h
p.51	TACCTCTAA	h.51.51	ATACCTCTAAGGGCCTTTTGGCCCTTAGAG GTATTTAGAGGTA/3InvdT/	0.6 µM	3 h
p.52	CTCCTATTT	h.52.52	ACTCCTATTTGGGCCTTTTGGCCCAAATAGG AGTAAATAGGAG/3InvdT/	0.3 µM	2 h
p.53	CTATCCAAA	h.53.53	ACTATCCAAAGGGCCTTTTGGCCCTTTGGAT AGTTTTGGATAG/3InvdT/	0.2 µM	3 h
p.54	ATCCCTATC	h.54.54	AATCCCTATCGGGCCTTTTGGCCCGATAGG GATTGATAGGGAT/3InvdT/	0.1 µM	3 h
p.55	TCATTACTT	h.55.55	ATCATTACTTGGGCCTTTTGGCCCAAGTAAT GATAAGTAATGA/3InvdT/	0.65 µM	3 h
p.56	CTAAATCTC	h.56.56	ACTAAATCTCGGGCCTTTTGGCCCGAGATTT AGTGAGATTTAG/3InvdT/	0.35 µM	3 h
Test-primer[29]	TCTCTTATT	h.test	ATCTCTTATTGGGCCTTTTGGCCCAATAAGA GATAATAAGAGA/3InvdT/	Not included in the gel assay	

The full set of 50 designed primer sequences are available in our recent work[30].

Supplementary Table 2. Bridge sequences used for antibody conjugation.

Bridge sequence index	DNA sequence
bc42_0	AATTCTATGACACCGCCACGCCCTATATCCTCGCAATAACCC
bc42_1	ATTATCCCTACCGCCAAATCTCCGTGTCCTTAACCGACCTAT
bc42_2	CGTTATCGCCGCCTTATCCACTGTACGATCCTATTCCTCTCC
bc42_3	GTTTCCTATATTTAGCGTCCGTGTCGTTCTCCCGCGCAACAG
bc42_4	TATCTTAAGTCTTCGCGTGTTGTCTCGTCTGGGTATTGCGTT
bc42_5	TCCTGTCCCGACGATCCTACCCTTAAAGTTACTGCGCACCCT
bc42_6	CGGTGAGGTAGGAGTCGTGCGTATCGTTTCCTATATAGCCGT
bc42_7	AGTTCCTGTAGTATCCCGTCGCATAGTCGTACATTCACCGTC
bc42_8	AACAATTCAGCTCCGCCTTATACCGTCTTACCGCCAACATCG
bc42_9	GAATTTGGCCCGTTCTATGTCTAACTCGTGTTCCCGCTTGTA
bc42_10	GTCCTCGCTCTTTCCGCATTTTCCCGTATGCGCTTTGTATTA
bc42_11	TGTCTAAATTCTAATGCCGCCCTATGCCGCCGTTCCAACAAT
bc42_12	CCTTCCGCCGTATGAATTTGACCCGAAGCCCAACCCGACCCT
bc42_13	CAGTTCTTGTATCGCGTCACTTATCGGTTATTGTCCTCTCGC
bc42_14	CCAACCTCTCGTACCAAATTCCGCCACTCAAGCCGTATCAAA
bc42_15	GTTTCAAGAGTCCGTCGCAAATTCCACTACACGCTACGCCCA
25mer-tester	TATTTAGTGTTCGAATAGTTCGATCTAG

The full set of 84 designed bridge sequences are available in our recent work[30]. For conjugation bridge oligos are designed as follows: /5ThioMC6-D/ tt (linker) bridge sequence (42mer).

Supplementary Table 3. Imager strands used for fluorescent visualization.

Imager ID	Imager sequence
i.25*	/Fluorophore/tt-TATTATTGG-t -ATTATTGG-t /3InvdT/
i.26*	/Fluorophore/tt-TAGGTTTAT-t-TAGGTTTAT-t /3InvdT/
i.27*	/Fluorophore/ tt-ATGATGATG-t-ATGATGATG-t 3InvdT/
i.28*	/Fluorophore/ tt-GTTAAGTTG-t-GTTAAGTTG-t/3InvdT/
i.29*	/Fluorophore/ tt-GATTTTAGA-t-GATTTTAGA-t/3InvdT/
i.30*	/Fluorophore/ tt-GAGAGTATT-t-GAGAGTATT-t/3InvdT/
i.31*	/Fluorophore/ tt-AGTGAATAA-t-AGTGAATAA-t/3InvdT/
i.32*	/Fluorophore/ tt-GAAAAAAAG-t-GAAAAAAAG-t/3InvdT/
i.33*	/Fluorophore/ tt AATAGAAGGt AATAGAAGG-t /3InvdT/
i.34*	/Fluorophore/ tt-GTAGTAGAG-t-GTAGTAGAG-t /3InvdT/
i.35*	/Fluorophore/ tt-GAGTTTTTA-t-GAGTTTTTA-t /3InvdT/
i.36*	/Fluorophore/ tt-AGATTAGTT-t-AGATTAGTT-t /3InvdT/
i.37*	/Fluorophore/ tt-GAAGAGAAA-t-GAAGAGAAA-t /3InvdT/
i.38*	/Fluorophore/ tt-TAGTATGTT-t-TAGTATGTT-t /3InvdT/
i.39*	/Fluorophore/ tt-GTAAATGAA-t-GTAAATGAA-t /3InvdT/
i.40*	/Fluorophore/ tt-TTGTAGGAT-t-TTGTAGGAT-t /3InvdT/
i.41*	/Fluorophore/ tt-TTTTGATTG-t-TTTTGATTG-t /3InvdT/
i.42*	/Fluorophore/ tt-GTTTGTAAG-t-GTTTGTAAG-t /3InvdT/
i.43*	/Fluorophore/ tt-GTTATTTGT-t-GTTATTTGT-t /3InvdT/
i.44*	/Fluorophore/ tt-GGTAGAAAA-t-GGTAGAAAA-t /3InvdT/
i.45*	/Fluorophore/ tt-AAATAAGGG-t-AAATAAGGG-t /3InvdT/
i.46*	/Fluorophore/ tt-AATGAAAGA-t-AATGAAAGA-t /3InvdT/
i.47*	/Fluorophore/ tt-GAGTAAGAA-t-GAGTAAGAA-t /3InvdT/
i.48*	/Fluorophore/ tt-GATTTATGG-t-GATTTATGG-t /3InvdT/
i.49*	/Fluorophore/ tt-GGATAAATG-t-GGATAAATG t /3InvdT/
i.50*	/Fluorophore/ tt-GTGAAGTAT-t-GTGAAGTAT t /3InvdT/
i.51*	/Fluorophore/ tt-TTAGAGGTA-t-TTAGAGGTA-t /3InvdT/
i.52*	/Fluorophore/ tt-AAATAGGAG-t-AAATAGGAG-t /3InvdT/
i.53*	/Fluorophore/ tt-TTTGGATAG-t-TTGGATAG-t /3InvdT/
i.54*	/Fluorophore/ tt-GATAGGGAT-t-GATAGGGAT-t /3InvdT/
i.55*	/Fluorophore/ tt AAGTAATGA-t-AAGTAATGA t /3InvdT/
i.56*	/Fluorophore/ tt GAGATTTAG-t-GAGATTTAG t /3InvdT/
Test-imager	/Fluorophore/ tt-AATAAGAGA-t-AATAAGAGA-t /3InvdT/

Supplementary Table 4. Antibodies used in SABER experiments, conjugated bridge sequences and respective SABER primers.

Antibody target	Source	Bridge sequence (for conjugation)	Capture and Toehold sequences for purification (if purified)	SABER primer sequences used in the experiments (+ denotes branching)
Cone arrestin	Millipore #AB15282	25mer-tester	Capture: Biotin-GTTGCTGTCGTATGT-CTAGATCGAACTATTC Toehold: GAATAGTTCGATCTAG-ACATACGACAGCAAC	p.30 (Fig. 2) or p28 + p25 (Supplementary Fig. 3) or test-primer (Fig. 5)
GFAP	ThermoFisher #13-0300	bc42_1	Capture: Biotin - GGGTAGGGTAGTGGT-ATAGGTCGGTTAAGGA Toehold: TCCTTAACCGACCTAT-ACCACTACCCTACCC	p.36 (Fig. 5 and 6)
PKCα	Novus #NB600-201	bc42_2	Binding sequence: Biotin - CGAGTGAGGTGGAAT-GGAGAGGAATAGGATC Toehold sequence: GATCCTATTCCTCTCC-ATTCCACCTCACTCG	p.25 (Fig. 5)
SV2	HybridomaBank Antibody Registry ID: AB_2315387	bc42_3	Capture: Biotin - CGAGTGGTAAGGCAT-CTGTTGCGCGGGAGAA Toehold: TTCTCCCGCGCAACAG-ATGCCTTACCACTCG	p.26 (Fig. 5, 6, Supplementary Fig. 8-9); or p27 + p28 + p32 (Supplementary Fig. 3)
Collagen IV	Novus #NB120-6586	bc42_4	Capture: Biotin - GAAATAGAATGAACG-AACGCAATACCCAGAC Toehold: GTCTGGGTATTGCGTT-CGTTCATTCTATTTC	p.27 (Fig. 2, 5 and 6)
Rhodopsin	EnCor Bio #MCA-A531	bc42_7	Capture: Biotin - GTTAAGGTGGAATGA-GACGGTGAATGTACGA Toehold: TCGTACATTCACCGTC-TCATTCCACCTTAAC	p.33 (Fig. 5 and 6)
Calbindin	EnCor Bio #MCA-5A9	bc42_8	Capture: Biotin - GGTGAGGTGTAGTGG-CGATGTTGGCGGTAAG Toehold: CTTACCGCCAACATCG-CCACTACACCTCACC	p.34 (Fig. 5)
Vimentin	Cell Signaling #5741S	bc42_9	Capture: Biotin - CGGAACAGATAAAGA-TACAAGCGGGAACACG Toehold: CGTGTTCCCGCTTGTA-TCTTTATCTGTTCCG	p.28 (Fig. 2. 5 and 6)
Calretinin	EnCor Bio #MCA3G9	bc42_10	Capture: Biotin - GCCAAATTCCACCGC-TAATACAAAGCGCATA Toehold: TATGCGCTTTGTATTA-GCGGTGGAATTTGGC	p.30 (Fig. 5 and 6)
VLP1	EnCor Bio #MCA-2D11	bc42_11	Capture: Biotin - CGGATGATGAGGGTG-ATTGTTGGAACGGCGG Toehold: CCGCCGTTCCAACAA-TCACCCTCATCATCCG	p.39 (Fig. 5)
Alpha-Tubulin	ThermoFisher #MA1-80017	bc42_0	Capture: Biotin - GTTGAGTGAGGTTGA-GGGTTATTGCGAGGAT Toehold: ATCCTCGCAATAACCC-TCAACCTCACTCAAC	p.30 or p.30 + p.28
Ki-67	Cell Signaling #9129 (formulated in PBS)	bc42_1	Capture: Biotin - GGGTAGGGTAGTGGT-ATAGGTCGGTTAAGGA Toehold: TCCTTAACCGACCTAT-ACCACTACCCTACCC	p.41 + p.34 (Fig. 4c), or p.30 or p.30 + p.28 or p.30 + p.28 + p.25 (all other figures)
CD8a	Cell Signaling	bc42_2	Capture: Biotin - CGAGTGAGGTGGAAT-	p.40 + p.28 (Fig. 4c) or

	#85336 (formulated in PBS)		GGAGAGGAATAGGATC Toehold: GATCCTATTCCTCTCC-ATTCCACCTCACTCG	p.25 + p.31 (all other figures)
PD-1	Cell Signaling #43248 (formulated in PBS)	bc42_3	Capture: Biotin - CGAGTGGTAAGGCAT-CTGTTGCGCGGGAGAA Toehold: TTCTCCCGCGCAACAG-ATGCCTTACCACTCG	p.26 + p.39
IgA	Jackson #109-005-011	bc42_7	Unpurified	p.34 (Fig. 4a) or p.25 (Fig. 4c)
CD3e	Cell Signaling #85061 (formulated in PBS)	bc42_9	Capture: Biotin - CGGAACAGATAAAGA-TACAAGCGGGAACACG Toehold: CGTGTTCCCGCTTGTA-TCTTTATCTGTTCCG	p.27 + p.32
IgM	Jackson #709-006-073	bc42_11	Unpurified	p.39 (Fig. 4a) or p.35 (Fig. 4c)
Lamin B	Santa Cruz sc-6216	25mer-tester (conjugated onto anti-goat secondary antibody, Jackson ImmunoResearch # 705-005-147)	Unpurified	p.28 + p.25 (Supplementary Fig. 6)
Bassoon	Enzo ADI-VAM-#PS003	bc42_0 (conjugated onto anti-mouse secondary antibody, Jackson ImmunoResearch #715-005-151)	Unpurified	p.30 (Fig.6 and Supplementary Fig. 9)
Homer1b/c	ThermoFisher #PA5-21487	bc42_3 (conjugated onto anti-rabbit secondary antibody, Jackson ImmunoResearch #711-005-152)	Unpurified	p.26 (Fig. 6 and Supplementary Fig. 9)
Anti-rabbit IgG (to detect Ki-67 indirectly)	Jackson # 711-005-152	bc42_3	Unpurified	p.30 + p.28 (Fig. 3d-f, Supplementary Fig. 5f)

Antibodies used to validate colocalization of VLP1 and Calretinin in **Supplementary Fig. 8d-f** are Calretinin (SantaCruz #SC-365956; EnCor Bio #CPCA-Calret; EnCor Bio #MCA-3G9 AP), VLP1 (EnCor Bio #RPCA-VLP1; EnCor Bio #CPCA-VLP1; EnCor Bio #MCA-2D11).
Fluorophore-conjugated secondary antibodies used for reference imaging: anti-rat-Alexa647 (Thermo Fisher #A-21472), anti-rabbit-Alexa488 (Thermo Fisher #A-21206), anti-rabbit-Atto488 (Rockland #611-152-122S), anti-mouse-Alexa647 (Thermo Fisher #A-31571), anti-goat-Alexa647 (Thermo Fisher # A-21447), anti-rabbit-Alexa647 (Jackson ImmunoResearch, 711-605-152).

Supplementary Table 5. Quantification strands.

Sequence ID	Sequence	Experiment / Figure number
25mer-tester*-tt-p.28-a-p.28	CTAGATCGAACTATTCGAACACTAAATA-tt-CAACTTAAC-a-CAACTTAAC	SABER for cone arrestin - unamplified control (Fig. 2 and Supplementary Fig. 3)
25mer-tester*-tt-p.28	CTAGATCGAACTATTCGAACACTAAATA-tt-CAACTTAAC	Linear SABER for cone arrestin (Fig. 2 and Supplementary Fig. 3)
28*-t-28*-t-28*-ttt-p.25	GTTAAGTTG-t-GTTAAGTTG-t-GTTAAGTTG-ttt-CCAATAATA	Branched SABER for cone arrestin (Supplementary Fig. 3)
bc42_3*-tt-p.27-a-p.27	CTGTTGCGCGGGAGAACGACACGGACGCTAAATA TAGGAAAC-tt-CATCATCAT-a-CATCATCAT	SABER for SV2 - no amplification control (Supplementary Fig. 5)
bc42_3*-tt-p.27	CTGTTGCGCGGGAGAACGACACGGACGCTAAATA TAGGAAAC-tt-CATCATCAT	linear SABER for SV2 (Supplementary Fig. 5)
27*-t-27*-t-27*-ttt-p.28	ATGATGATG-t-ATGATGATG-t-ATGATGATG-ttt-CAACTTAAC	Branched SABER for SV2 (Supplementary Fig. 5)
28*-t-28*-t-28*-ttt-p.32	GTTAAGTTG-t-GTTAAGTTG-t-GTTAAGTTG-ttt-CTTTTTTC	Iterative SABER for SV2 (Supplementary Fig. 5)
bc42_2*-tt-p.25-a-p.25-a	GGAGAGGAATAGGATCGTACAGTGGATAAGGCG GCGATAACG-tt-CCAATAATA-a-CCAATAATA a	SABER for CD8a - unamplified control (Fig. 2 and Supplementary Fig. 3)
bc42_0*-tt-p.30-a-p.30-a	GGGTTATTGCGAGGATATAGGGCGTGGCGGTGTC ATAGAATT-tt-AATACTCTC-a-AATACTCTC a	SABER for Ki67 - unamplified control (Fig. 3 and Supplementary Fig. 5)
25mer-tester*-tt-a-p.27-a-p.27-a-p.28	CTAGATCGAACTATTCGAACACTAAATA-tt-a CATCATCAT-a-CATCATCAT-a-CAACTTAAC For 350-nt: 1 h reaction with 0.1 µM h.28.28.ip For 450-nt: 1 h reaction with 0.2 µM h.28.28.ip For 750-nt: 1 h reaction with 0.4 µM h.28.28.ip	Linear SABER for Lamin B - quantification strand (Supplementary Fig. 4)
28*-t-28*-t-28*-t-a-p.30-a-p.30-tt-p.25	GTTAAGTTG-t-GTTAAGTTG-t-GTTAAGTTG-t-a-AATACTCTC-a-AATACTCTC-tt-CCAATAATA For 250-nt: 1 h reaction with 0.05 µM h.25.25 For 450-nt: 1 h reaction with 0.15 µM h.25.25	Branched SABER for Lamin B - quantification strand (Supplementary Fig. 4)

Supplemental Notes

Supplemental Note 1. Antibody-DNA conjugations

Not all commercial antibodies are provided in a formulation readily available for conjugation (for example antibodies may be provided in unpurified whole serum form or formulated with stabilizers or protectors that interfere with conjugation). Hence customized formulation of antibodies may be required. In addition, we currently utilize non-specific conjugation to Lys residues and provide a simple protocol to prepare custom conjugation of antibodies (Agasti et al., Chem Sci, 2017; also see **Supplemental Protocols**). Although multiple DNA oligos can be attached to each antibody molecule for further signal amplification, our reaction conditions are optimized to achieve 1-3 oligos per antibody, to prioritize conserving the antigen recognition capability upon conjugation. Alternatively, site-specific conjugation chemistries could be utilized, including click labeling of antibody gylcosyl residues (available as the SiteClick™ kit from Thermo Fisher). Independent of the conjugation method, we recommend testing of antibodies after conjugation to ensure functionality through comparison of the staining pattern with unconjugated antibody. As the high potential of DNA barcoding gains higher recognition and visibility, commercial antibody-DNA conjugation services and ready-to-use kits are also becoming available. Additionally, alternative recent probes (recombinant antibodies, nanobodies, aptamers, etc.) and probe labeling methods (such as unnatural amino acid incorporation or engineering of site-specific adaptor molecules) could facilitate new and highly-efficient means for standardized large-scale probe libraries as future resources.

Ref: Agasti, S.S., Wang, Y., Schueder, F., Sukumar, A., Jungmann, R., & Yin, P. DNA-barcoded labeling probes for highly multiplexed Exchange-PAINT imaging. *Chemical Science*, *8*(4), 3080-3091 (2017).

Supplemental Note 2. Sample stability over time

A potentially important factor for reproducibility is the time between sample preparation and imaging. To enable easy washing for multiplexing, the imager binding is designed to be not extremely stable. When samples are kept in buffer (such as PBS) over extended periods, imagers might get lost over time. To avoid that, we recommend paying attention to this factor in experimental design, and either keeping the storage conditions and time similar in between experiments (for exchange imaging), or to use curing embedding media (such as ProLong Diamond) to keep the imagers from de-hybridizing and diffusing away (for spectral multiplexing without exchange) (also see **Supplemental Protocols – General recommendations**).

Supplemental Note 3: Tensorflow implementation hyperparameters for nuclear segmentation

We used our own implementation in TensorFlow with the following hyperparameters: Number of feature maps in first convolutional layer: 8; Number of feature maps in subsequent downsampling layers: 2 times the number of feature maps in previous layer; Downsampling and upsampling factor: 2; Convolution kernel size: 3; Number of extra convolutions in each layer: 1; Variance of truncated normal distribution generating initial random weights: 0.1; Number of downsampling layers: 2; Batch size: 8; Number of training steps: 20,000; Learning rate: initially 0.1, with 'staircase' exponential decay (step 1000, rate 0.95), and momentum 0.9.